

A robust relationship between multidecadal global warming rate variations and the Atlantic Multidecadal Variability

Zhiyu Li^{1,2} · Wenjun Zhang¹ · Fei-Fei Jin³ · Malte F. Stuecker⁴ · Cheng Sun⁵ · Aaron F. Z. Levine^{6,7} · Haiming Xu¹ · Chao Liu¹

Received: 17 January 2020 / Accepted: 6 July 2020 / Published online: 11 July 2020 © Springer-Verlag GmbH Germany, part of Springer Nature 2020

Abstract

How much and fast the Earth is warming in response to increasing greenhouse gas concentrations is one of the fundamental questions in climate science. Here we investigate the role that different modes of climate variability play in modulating the temperature response. We show evidence for a robust statistical relationship between global warming rate variations and Atlantic Multidecadal Variability (AMV) across multiple observational datasets since 1850. The correlation between AMV and the global warming rate is maximized—with a correlation coefficient of about -0.8—at ~ 10 to 20 years lead-time. In contrast, such a relation between global warming rate and the Interdecadal Pacific Oscillation (IPO) is far less coherent, showing negative correlation before the 1920s and positive correlation after that. Similar statistical relationships between global warming rate variations and the AMV/IPO can also be seen in the majority of the models from the Phase 5 of Coupled Models Inter-comparison Project. Further, a targeted model experiment is conducted to demonstrate the dominant control of the AMV on the unforced fraction of the global warming rate (compared to the IPO).

Keywords Global warming rate · AMV · IPO · Multidecadal timescale

- Wenjun Zhang zhangwj@nuist.edu.cn
- CIC-FEMD/ILCEC, Key Laboratory of Meteorological Disaster of Ministry of Education (KLME), School of Atmospheric Sciences, Nanjing University of Information Science and Technology, Nanjing 210044, China
- Guizhou Meteorological Observatory, Guizhou Meteorological Bureau, Guiyang, China
- Department of Atmospheric Sciences, SOEST, University of Hawai'i at Mānoa, Honolulu, HI, USA
- Department of Oceanography and International Pacific Research Center, School of Ocean and Earth Science and Technology, University of Hawai'i at Mānoa, Honolulu, HI, USA
- College of Global Change and Earth System Science, Beijing Normal University, Beijing, China
- ⁶ NOAA/PMEL, Seattle, WA, USA
- Department of Atmospheric Science, University of Washington, Seattle, WA, USA

1 Introduction

Observations show that global mean atmospheric surface temperature (GMST) have increased by ~0.85 [0.65–1.06] °C since the beginning of the Industrial Revolution (1880–2012) due to steadily increasing anthropogenic greenhouse-gas concentrations (IPCC 2013). However, the GMST has not increased at a constant rate over this period due to a combination of time-varying forcing and internal variability (e.g., Wu et al. 2007; Tung and Zhou 2015; Wei et al. 2019). Recently, a transient slowdown of the warming rate, which was coined "global warming hiatus", occurred during the first decade of the 21st century. It has been a focal point of research activity and various mechanisms explaining its occurrence have been proposed (e.g., Kosaka and Xie 2013; Chen and Tung 2014, 2018; McGregor et al. 2014; Medhaug et al. 2017). Some studies emphasized the role of external forcing and feedbacks, such as the changes in stratospheric and tropospheric aerosols and decreased stratospheric water vapor during recent decades (Solomon et al. 2011; Fyfe et al. 2013; Santer et al. 2014; Takahashi and Watanabe 2016). In contrast, others stressed the contribution of natural variability from the El Niño-Southern



Oscillation (ENSO; Bjerknes 1969) and major decadal climate modes, such as the Interdecadal Pacific Oscillation (IPO; Power et al. 1999)/Pacific Decadal Oscillation (PDO; Mantua et al. 1997) and the Atlantic Multidecadal Variability (AMV; Knight et al. 2005), in modulating the global warming rate (Fyfe et al. 2013; Kosaka and Xie 2013; Trenberth and Fasullo 2013; Chen and Tung 2014, 2018; England et al. 2014; Gleisner et al. 2015; McGregor et al. 2014; Medhaug et al. 2017).

The IPO index describes dominant interdecadal variability of sea surface temperatures (SSTs) in the Pacific. The associated spatial pattern is characterized by positive SST anomalies in the tropical eastern Pacific and negative SST anomalies in the Northwest and Southwest Pacific during its positive phase and vice versa during its negative phase (Power et al. 1999; Parker et al. 2007; Henley et al. 2015). The IPO has been proposed as one key factor for the recent hiatus as its phase transition from positive to negative around the late 1990s corresponds well with the start of the hiatus period (e.g., Trenberth and Fasullo 2013; England et al. 2014; Tollefson 2014; Dai et al. 2015; Medhaug and Drange 2016). The increased ocean heat content over the tropical Pacific below 700 m during recent decades provides support to the idea that the tropical Pacific plays an important role in the hiatus phenomenon (e.g., Katsman and Oldenborgh 2011; Guemas et al. 2013; Medhaug and Drange 2016). Additionally, enhanced heat storage during this period was observed in the Indian Ocean, supplemented by increased heat transport from the Pacific Ocean via the Indonesian throughflow (Drijfhout et al. 2014; Lee et al. 2015; Nieves et al. 2015; Liu et al. 2016). In addition, the AMV has been proposed as another potential contributor to the recent global warming hiatus. A positive phase of the AMV is characterized by basin wide positive SST anomalies over the North Atlantic and a negative AMV phase by a basin-wide cooling. Some scientists argued that changes in North Atlantic heat-sequestration could have played some role (Chen and Tung 2014, 2018). Other studies proposed that both IPO and AMV contribute to global mean surface temperature variability and ocean heat redistribution in similar magnitude (Drijfhout et al. 2014; Huang et al. 2016). In addition, it has been proposed that the AMV can affect the global warming rate through its indirect remote influence on the IPO, especially during the hiatus period (McGregor et al. 2014; Chikamoto et al. 2016; Li et al. 2016; Ruprich-Robert et al. 2017). At present, the relationship between these modes of climate variability and the recent warming hiatus is still strongly debated, partly due to different definitions and methodologies and due to the relatively short observational temperature record relative to (multi-)decadal climate variability timescales. Moreover, the physical mechanisms determining the IPO and AMV patterns and time evolution are strongly debated as well (e.g., Zhang et al. 2013; Clement et al. 2015; Wills et al. 2019). For instance, whether low-frequency climate variability in the Pacific and Atlantic basins are actual oscillations (associated with characteristic timescales) or autoregressive processes of order one (AR(1)) forced by stochastic noise can to date not be answered satisfactorily given the length of the observational temperature record (see for instance discussions in Newman et al. 2016 and Mann et al. 2020). The role of external forcing explaining part of the variance associate with these statistical modes is also debated, especially for the AMV. For instance, anthropogenic aerosols are proposed to modulate the observed AMV (e.g., Booth et al. 2012; Clement et al. 2015; Murphy et al. 2017), while others argue that internal variability associated with the Atlantic Meridional Overturning Circulation (AMOC) is predominant (e.g., Bjerknes 1964; Kushnir 1994; Delworth et al. 1993; Ting et al. 2009, 2014; Danabasoglu et al. 2012; Zhang et al. 2013; McCarthy et al. 2015; DelSole et al. 2010). The distinction between these has important implications for potential predictability of climate variability on decadal timescales.

As mentioned earlier, the global warming rate exhibits multidecadal fluctuations (e.g., Wu et al. 2007; Li et al. 2013; Tung and Zhou 2015; Wei et al. 2019). Warming hiatuses can be observed over different periods, such as 1880s-1910s and 1940s-1970s, whereas warming surges can be seen during 1910s-1940s and 1970s-2000s. The association of the recent hiatus with internal variability has been a motivation to explore to which extent natural variability drives global warming rate changes (hiatuses/surges) on multidecadal timescales on top of the secular trend driven by increasing greenhouse gas concentrations. Recent studies argued that the IPO dominates the global warming rate on interdecadal timescales (Kajtar et al. 2019; Wei et al. 2019), especially in recent decades (Steinman et al. 2015). This includes the global warming hiatus, which has been associated with IPO associated internal variability (Kosaka and Xie 2013; Trenberth and Fasullo 2013; England et al. 2014; Tollefson 2014; Dai et al. 2015; Medhaug and Drange 2016). However, the relationship between the IPO and global warming rate variations on longer (multidecadal) timescales is still an open question. Recent work emphasizes that the AMV might play a larger role than the IPO for the multidecadal internal variability imprint on the GMST during most of the twentieth century (Chylek et al. 2016; Stolpe et al. 2017; Young-Min et al. 2019). At present, the general relationship between AMV/IPO and the global warming rate variations is still unclear and needs further attention. In this study, we revisit the statistical relationship between global warming rate variations and the AMV and IPO on multidecadal timescales, based on multiple observational records since 1850 as well as CMIP5 model simulations. Our results show a robust stationary statistical relationship between global warming rate variations and the AMV on



multidecadal timescales while the relationship with the IPO is far less coherent. Additionally, a climate model experiment with an idealized sinusoidal AMV forcing further substantiates this conclusion.

In the remainder of the paper, Sect. 2 introduces data, methods and our experimental design. Section 3 reports relationships of global warming rate with the AMV and IPO in observations. Next, the relationships are examined in the CMIP5 multi-model ensemble and with a targeted model experiment in Sect. 4. The major conclusions are summarized and discussed in Sect. 5.

2 Data and methodology

2.1 Data and methodology

The sea surface temperatures were obtained from the National Oceanic and Atmospheric Administration (NOAA) Extended Reconstructed SST version 4 (ERSST v4; Huang et al. 2015). In this study, the AMV index is defined as the SST anomalies averaged over the northern Atlantic (0°–70° N, 0°–90° W, AMV1). An "unforced" AMV index (Fig. 3; AMV2) was calculated by removing the multi-model mean of 28 CMIP5 historical simulations which are extended to 2017 with the RCP 8.5 simulations (Riahi et al. 2011). The RCP8.5 experiments were often used to extend the historical simulations (e.g., Schmidt et al. 2014; Frankignoul et al. 2017; Kajtar et al. 2019). The results of RCP4.5 experiments were also examined and there was only a small difference between them (not shown), which is expected as the radiative forcing between the two pathways is small during the

first few years and only becomes distinct later in the 21st century. This method relies on each model having the same response to the external forcing, which is not necessary a good assumption (Frankcombe et al. 2015). While the secular trend is the dominant component, we emphasize that it is difficult to fully separate the internal and external variability on shorter (i.e., decadal) timescales over the observational record. The models are listed in Table 1. Three models (BNU-ESM, CESM1-WACCM, and MPI-ESM-P) are not used as their RCP 8.5 simulations were unavailable. We also tested the effect of removing the multi-model mean of the subset of 25 CMIP6 historical simulations which range from 1850 to 2014 and the results did not change significantly (not shown). The IPO index is defined as $IPOI = [SST]_{FO} - ([SST]_{FO} -$ T_{NW} +[SST]_{SW})/2 (Henley et al. 2015), where the brackets represent the area-averaged SST anomalies over the region of the tropical eastern Pacific (EQ: 10° S-10° N, 170°-90° W), the Northwest Pacific (NW: 25°-45° N, 140° E-145° W), and the Southwest Pacific (SW: 50°-15° S, 150° E-160° W) respectively. An "unforced" IPO index was also calculated, and it shows little difference with the original one $(R = \sim 1.0; \text{ not shown})$. The monthly surface temperature data used was obtained from the Cowtan and Way global mean temperature dataset (Cowtan and Way 2014; http:// www-users.vork.ac.uk/~kdc3/papers/coverage2013/serie s.html), the Goddard Institute for Space Studies dataset (GISS; Hansen et al. 2010), and the NOAA GlobalTemp dataset (Vose et al. 2012). To avoid the underestimation of temperature trend caused by coverage bias (Cowtan and Way 2014; Karl et al. 2015), the Cowtan and Way dataset interpolates Hadley Centre-Climatic Research Unit Temperature (HadCRUT; Morice et al. 2012) to global coverage. The

Table 1 The leading year of the maximum correlation between the AMV and global warming rate for preindustrial control simulations from 31 CMIP5 models

Model name	Leading year	Length of simulation	Model name	Leading year	Length of simulation
ACCESS1-0	6	500	GISS-E2-H-CC	10	251
bcc-csm1-1-m	6	400	GISS-E2-R	8	251
BNU-ESM	7	559	GISS-E2-R-CC	10	251
CanESM2	6	996	HadGEM2-ES	8	577
CCSM4	7	501	inmcm4	7	500
CESM1-WACCM	6	200	IPSL-CM5A-LR	8	1000
CMCC-CESM	9	277	IPSL-CM5A-MR	8	300
CMCC-CM	7	330	IPSL-CM5B-LR	9	300
CMCC-CMS	8	500	MIROC5	8	670
CNRM-CM5	11	850	MPI-ESM-LR	7	1000
CSIRO-Mk3-6-0	8	500	MPI-ESM-MR	6	1000
EC-EARTH	8	452	MPI-ESM-P	8	1156
FIO-ESM	7	800	MRI-CGCM3	8	500
GFDL-ESM2G	10	500	NorESM1-M	5	501
GFDL-ESM2M	7	500	NorESM1-ME	9	252
GISS-E2-H	6	1770			



GMST was calculated from the Cowtan and Way data unless otherwise specified. The ERSSTv4 dataset cover the period 1860–2017, Cowtan and Way dataset cover 1850–2017, and both GISS and NOAA GlobalTemp data cover 1880–2017. We also examined the relationship of global warming rates with the AMV and IPO in the historical and pre-industrial control simulations from 31 CMIP5 models (http://cmip-pcmdi.llnl.gov/cmip5/index.html).

Anomalies for all variables were computed as the deviation from the long-time climatological mean (1961–1990). As the forced response can be better modeled as a quadratic trend rather than a linear trend (Wu et al. 2007; Frankcombe et al. 2015; Mann et al. 2014), we first remove the quadratic trend from all data. Then we apply a 13-year lowpass Lanczos filter (Duchon, 1979) on all data to focus on multidecadal variability (except for the GMST anomalies in Fig. 12a). In addition, 9-year and 17-year low-pass filters are also tested, and the results are almost the same. Different windows used in the low-pass filter do not affect our conclusion. Warming rates are calculated as a trend in a sliding 21-year window defined at the centered year of the window. To avoid the possible contribution of North Atlantic SSTs to the GMST estimation, the adjusted global warming rate in Fig. 2 is defined as 21-year sliding trends of global averaged (excluding North Atlantic basin [0°-70° N, 0°-90° W]) surface temperature. We also calculated the trend in sliding 11-year and 31-year windows and the results did not change significantly (not shown). All statistical significance tests were performed using the two-tailed Student's t test. The effective number of degrees of freedom, n, was computed and we removed the influence of autocorrelation on the correlation significance (Davis 1976), which was determined by the theoretical approximation $n = \frac{N}{T}$, where N is the sample size and $T = \sum_{j=-\infty}^{\infty} R_{xx}(j)R_{yy}(j)$ (Rxx(j)) and Ryy(j) are the autocorrelations of two sampled time series X and Y. The false discovery rate (FDR) test was also applied to deal with the multiplicity problem in our study (Wilks 2016).

2.2 Experimental design

To further examine the impact of the AMV on the global warming rate, a 500-year model experiment was conducted using the Geophysical Fluid Dynamics Laboratory (GFDL) coupled model (CM2Mc; Galbraith et al. 2011) with a general setup similar to Levine et al. (2017). The atmospheric and oceanic component, respectively, has 3.5° longitude $\times 3^{\circ}$ latitude horizontal resolution with 24 vertical levels and nominal 3 degree ocean resolution increasing to $\sim 0.6^{\circ}$ at the equator with 28 vertical levels. In the AMV-forced experiments, North Atlantic SSTs ($10^{\circ}-80^{\circ}$ W, $0^{\circ}-70^{\circ}$ N) are relaxed to the monthly climatology plus a 50-year sinusoidal varying AMV-related SST anomaly. The AMV anomaly was calculated by regressing Simple Ocean Data Assimilation

(SODA) version 2.2.4 (Giese and Ray 2011) SSTs on the normalized Earth System Research Lab AMV index (https ://www.esrl.noaa.gov/psd/data/timeseries/AMO/). The SST relaxation timescale is 2 days and the associated reference depth is 10 meters and the SSTs are allowed to evolve freely outside of the prescribed regions. Similar relaxing time can also be seen in other studies (Dong et al. 2006; Lu et al. 2006; Levine et al. 2017, 2018). We also conducted the experiment with a 4-day relaxation timescale and the conclusions are almost the same despite of slightly weaker impact of the AMV on the global warming rate. We here choose the 50-year timescale for the AMV variability as a compromise between the observed timescale of Atlantic multidecadal variability and computational costs. The 50-year AMV periodicity in our simulations does not influence the simulated climate responses to the AMV (Levine et al. 2017, 2018) and our qualitative conclusions. When reconstructing the global warming rate based on the idealized AMV-forced experiment (Fig. 11), the experimental results are multiplied by a scaling factor of 0.475 (ratio between observed and prescribed AMV amplitude in model) assuming a quasi-linear response owing to relative weak forcing amplitude.

3 Relationships of the global warming rate with the AMV and IPO in observations

We here report that the statistical relationships between global warming rate variability and the AMV/IPO are substantially different from each other during the extended observational record since 1850. The lead/lag correlations of the global warming rate with the AMV and IPO show that AMV changes tend to lead global warming rate changes within a range of 10-20 years (the year of maximum correlation is 12 with a correlation coefficient of -0.81), while no statistically significant correlations can be found between the IPO and the global warming rate at different lead times (Fig. 1). We hereafter focus on the 12-year lead relation between the AMV and the global warming rate in the remainder of the manuscript. Since the simultaneous relationships between the IPO and global warming rate was mentioned in many previous studies (e.g., Kosaka and Xie 2013; Trenberth and Fasullo 2013; England et al. 2014; Tollefson 2014; Dai et al. 2015; Medhaug and Drange 2016), the simultaneous relationship between the IPO and global warming rate is analyzed here. We focus on possible modulations of the main SST modes on the GWR variability, thus any marginally significant lag correlations are not considered in this study. From investigating the time series of global warming rate, the AMV (at 12-year lead), and IPO (Fig. 2), it is evident that the multidecadal variations of the global warming rate correspond well with AMV phase transitions throughout the entire period. The IPO phase transitions



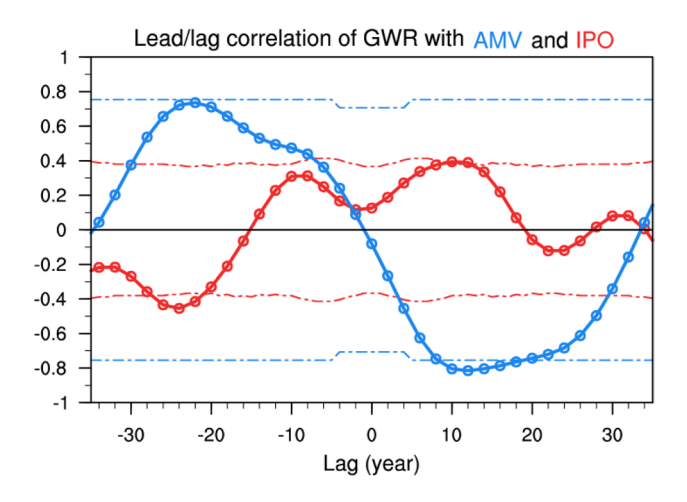


Fig. 1 Cross correlations between the global warming rate and AMV (blue)/IPO (red). Positive (negative) years on the x-axis indicate that the AMV/IPO leads (lags) the global warming rate. The blue and red dashed lines indicate the 95% confidence level of the correlation coefficients for AMV and IPO indices, respectively

also correspond to GMST warming and cooling episode transitions after the 1920s, consistent with previous studies (Tollefson 2014; Dai et al. 2015; Trenberth 2015). However, we see the opposite relationship before the 1920s, resulting in an unstable statistical relationship between global warming rate and IPO over the 158-years record.

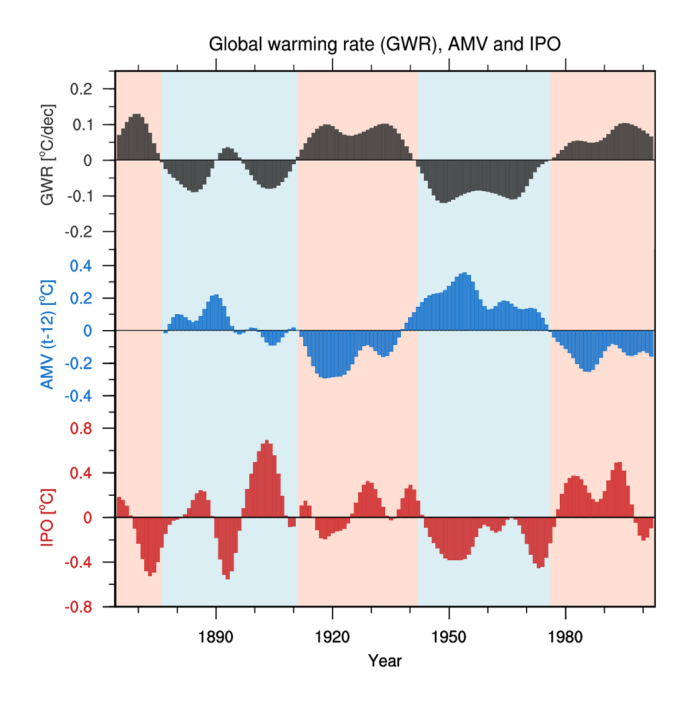


Fig. 2 Time series of the global warming rate (black in °C/decade), and indices of AMV (the AMV is shifted forward by 12 years; blue in °C) and IPO (red in °C)

Previous studies argued that the traditional AMV index might include the influence of anthropogenic forcing (Booth et al. 2012). To exclude the possible forced signal, we here calculate the unforced AMV index based on the method of Kajtar et al. (2019). After removing the multi-model mean of 28 CMIP5 historical simulations (not shown) from the observed AMV index, the unforced AMV is still statistical significantly correlated with the global warming rate (R = -0.78; Fig. 3a). We also recalculated the global warming rate by excluding the North Atlantic basin (0°-70° N, $0^{\circ}-90^{\circ}$ W) and found similar results (R = -0.82 between global warming rate and AMV; Fig. 3b). To check whether these statistical relationships are robust over the entire period, the 45-years sliding correlations of the global warming rate with the AMV and IPO are calculated respectively (Fig. 4a). All of the three historical records consistently show that the correlation between global warming rate and the AMV is largely stationary (R = -0.68 for 1877–1926 and R = -0.90 for 1927–2002 based on the Cowtan and Way and ERSST datasets), while the correlation with the IPO reverses its sign before and after the 1920s, leading to

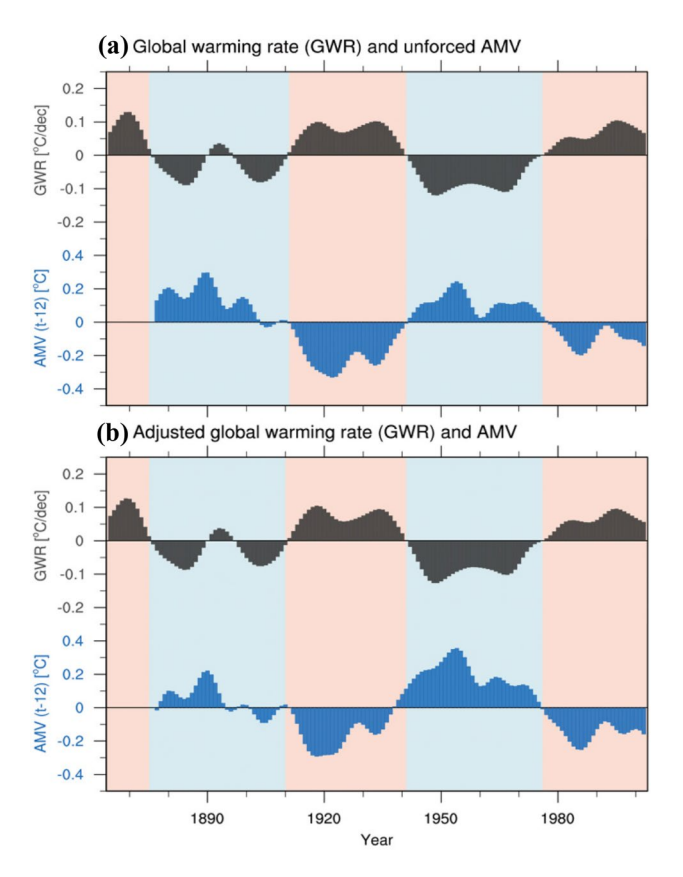


Fig. 3 a Time series of the global warming rate (black in °C/decade), and the unforced AMV index (blue in °C). **b** Time series of the adjusted global warming rate (global average but excluding the North Atlantic basin (0°–70° N, 0°–90° W); black in °C/decade) and AMV index. The AMV indices in **a**, **b** are shifted forward by 12 years



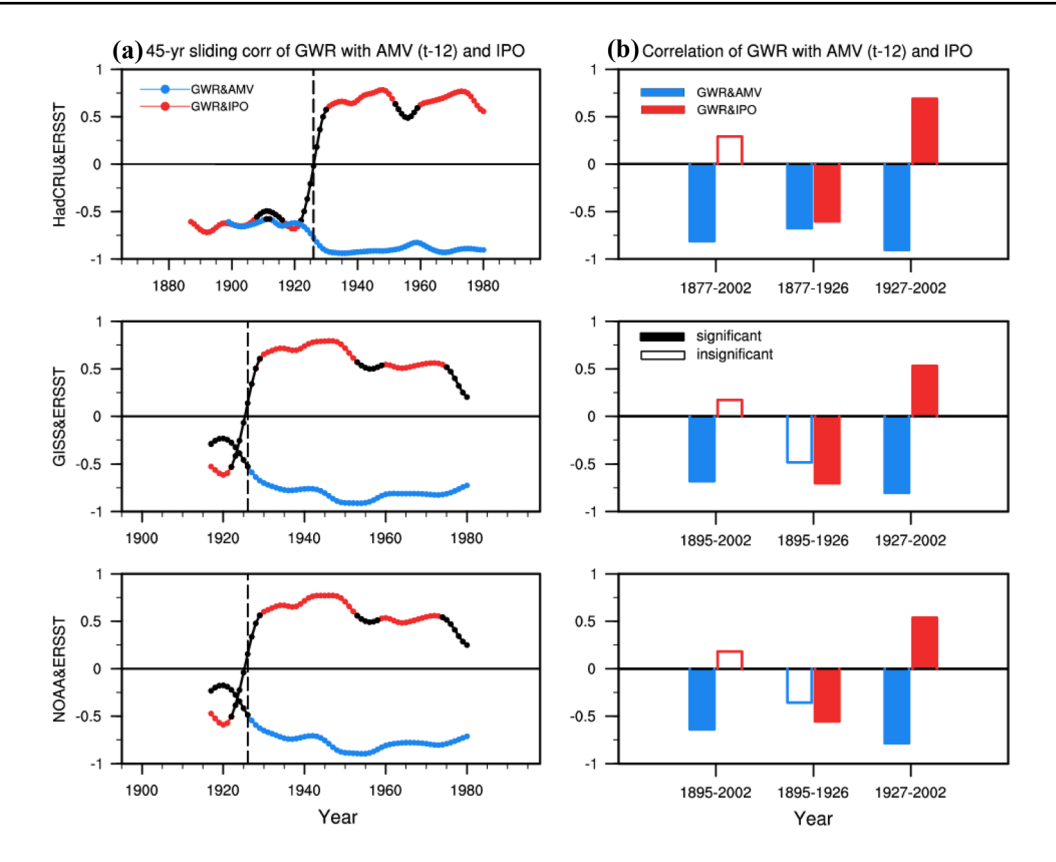


Fig. 4 a 45-year sliding correlation coefficients between the global warming rate and the IPO (red and black) and AMV (AMV is leading the global warming rate by 12 years; blue and black). Colors (red and blue) in the solid curves indicate correlation coefficients exceeding the 95% confidence level. The vertical dashed line marks the year (1926) for the transition of the statistical relationship between the IPO and global warming rates. b Correlation coefficients between the global warming rate and IPO (red) and AMV index (blue) during

1877–1998, 1877–1926, and 1927–1998. Filled bars in **b** indicate statistical significance at the 95% confidence level. The global warming rate is calculated based on the HadCRU (upper row), GISS (middle row), and NOAA (lower row) data, respectively. The IPO and AMV indices are derived from the ERSST data. The results based on the GISS and NOAA data are derived from 1895 onwards due to the shorter data period

a statistically insignificant correlation over the entire period (R=-0.60 for 1877-1926, R=0.69 for 1927-2002, and R=0.29 for 1877-2002; Fig. 4b). 51-years sliding correlations are also tested and the results remain the same despite some differences (not shown).

The global warming rate can be mathematically understood as the first derivative of the GMST. We argue that there exists about 1/4 phase shift or 1/4 time lead/lag of their dominant periodicity between the two time series. As the AMV index shows high simultaneous correlation with the detrended GMST (Fig. 5a), there may exist ~12-year lead correlation between the AMV and the global warming rate. The AMV induced surface temperature anomalies feature a spatially uniform warming over almost all regions north of ~30° S (Fig. 5b). Similar patterns can also be detected in other observational records, with some uncertainties over

the North Pacific as well as the tropical central and eastern Pacific (Fig. 6). Consistently, a large-scale cooling pattern is evident for the regression coefficient of the surface temperature warming rate anomalies upon the normalized AMV at a 12-year lead, especially over the North Hemisphere. Some statistically insignificant signals are again evident over the North Pacific as well as the tropical central and eastern Pacific (Fig. 7a).

In contrast, the surface temperature anomalies associated with the IPO index exhibit a distinct tripole pattern in the Pacific (Fig. 8). Surface temperatures in regions around the Pacific, such as North America and northeast Australia, and even the Eurasian mid-latitudes are affected by the IPO, which is consistent with previous studies (e.g., Meehl et al. 2016; Dai 2013; Dong and Dai 2015). The averaged GMST during different IPO phases are also examined. There is no



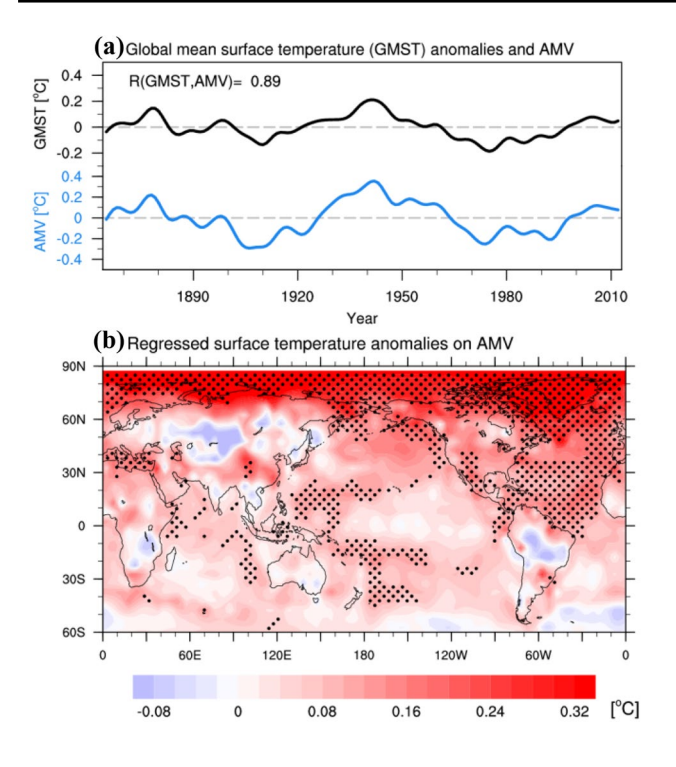
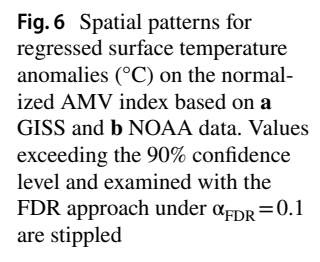


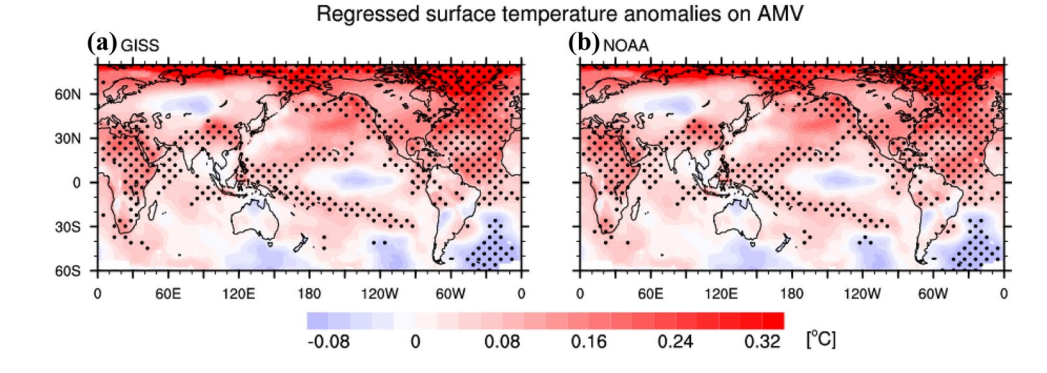
Fig. 5 a Time series of the global mean surface temperature anomalies (black in °C) and AMV index (blue in °C). **b** Linear regression pattern of the surface temperature anomalies (°C) to the normalized AMV index. Values exceeding the 90% confidence level and examined with the FDR approach under $\alpha_{FDR}\!=\!0.1$ are stippled

evident relationship between the IPO and GMST variability, and the related GMST responses are weak and statistically insignificant except for the period of 1924–1944 (not shown). As for the global warming rate, only a few regions show a statistically significant simultaneous relationship between the IPO and surface temperature warming rates, even over the Pacific (Fig. 7b). Thus, it seems that the AMV rather than the IPO has a strong and robust stationary statistical relationship with the global warming rate on multidecadal timescales.

We emphasize here that it is difficult to fully remove the effect of external forcing from the observational temperature

We emphasize here that it is difficult to fully remove the effect of external forcing from the observational temperature record. To further support our conclusions, we examine several AMV definitions, such as removing the simultaneous global mean temperature from the SST between 25°–60° N and 7°–75° W (van Oldenborgh et al. 2009; AMV3), removing the simultaneous SST between 60°S–60° N from the SST over 0°–60° N and 0°–80° W (Trenberth and Shea, 2006; AMV4), as well as the multidecadal component of the North Atlantic (0°–70° N, 0°–90° W) SST anomaly decomposed with the multidimensional (ensemble) empirical mode decomposition (EMD or EEMD; Wu et al. 2007; AMV5). We also employed different methods to exclude the external forcing effect, such as linear (Enfield et al. 2001; AMV6), nonlinear detrending (Enfield and Cid-Serrano 2010; AMV1), removing the regressed SST anomaly at each grid





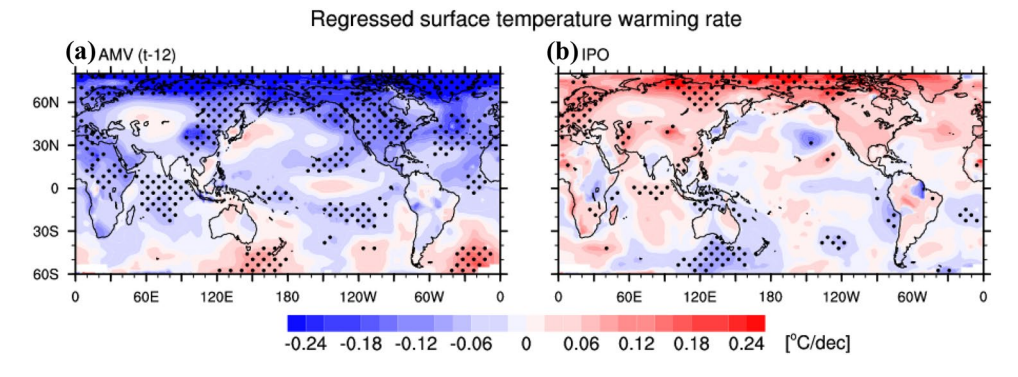


Fig. 7 Spatial patterns for regressed surface temperature warming rate (°C/decade) on the normalized **a** AMV and **b** IPO indices. The regression is calculated when the AMV leads the surface temperature warming rate by 12 years in **a**. Values exceeding the 90% confidence

level and examined with the FDR approach under $\alpha_{FDR}\!=\!0.1$ are stippled. The surface temperature warming rate is calculated based on the GISS data from 1880 to 2013 due to relatively good data coverage during that period



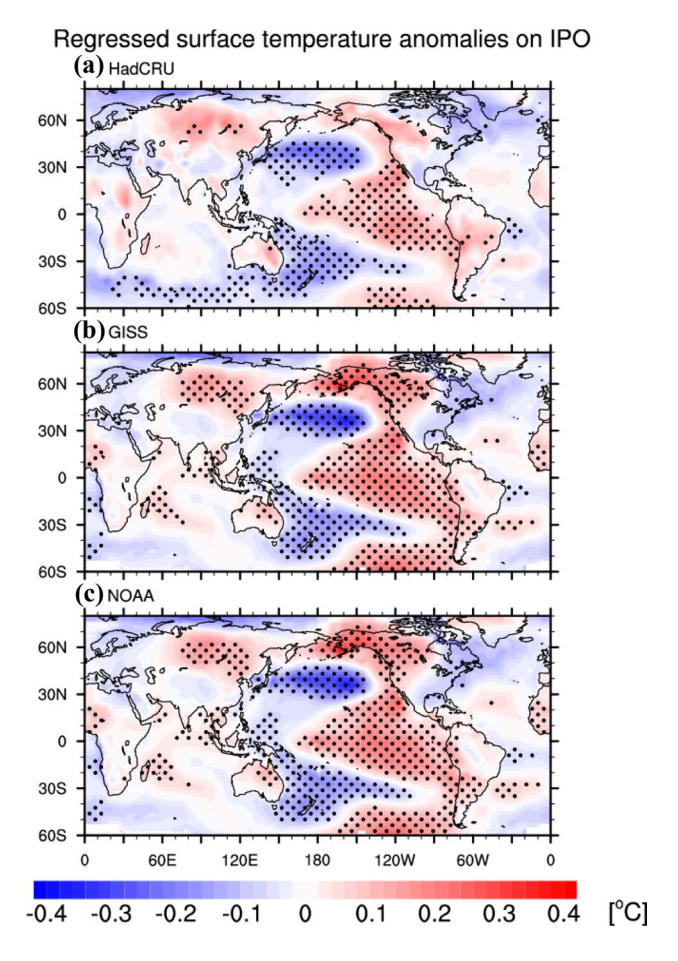


Fig. 8 Spatial patterns for regressed surface temperature anomalies (°C) on the normalized IPO index based on a HadCRU, b GISS, and c NOAA data. Values exceeding the 90% confidence level and examined with the FDR approach under $\alpha_{\text{FDR}} = 0.1$ are stippled

point on the yearly global mean SST anomaly (Frankignoul et al. 2017; AMV7), and removing the multi-model mean of the historical simulations (AMV2). All of the different definitions and methods result in a statistically significant relationship between the AMV and global warming rate in the observations (Table 2). The qualitative conclusions are not affected by our definition of the AMV and the estimation of the external forcing.

4 Relationships of global temperature rate variations with the AMV and IPO in climate models

The relatively short (i.e., with respect to resolving multidecadal timescale variability) global climate records regrettably only provide a small sample size to investigate the statistical relationship between AMV/IPO and multidecadal fluctuations of the global temperature rate. The observed relationships between them is also challenged by the uncertainty of the SST reconstructions before the 1950s, especially in the Pacific Ocean (Deser et al. 2010). Therefore, we further examine the relationships between global temperature rate changes and these two modes of climate variability in preindustrial control simulations in 31 climate models participating in CMIP5 (Table 1). In these simulations, the external forcing (e.g., greenhouse-gas, aerosols, solar, and volcanic forcing) is kept constant and thus our analyses reflect purely internal climate variability.

Figure 9 shows the statistical relationships between AMV, IPO, and the global temperature rate in these state-of-theart coupled models. Almost all of the models exhibit significant negative correlations (all above the 95% confidence level except for one model) between the AMV and global temperature rate that are maximized at ~5 to 11-year leadtime (ensemble mean = 8 years; Table 1, Fig. 9a). Despite different performances in simulated AMV variability by various coupled models, they consistently capture the statistically significant relationship between AMV variability and global temperature rate variations despite a weaker correlation compared with the observations. The surface temperature rate associated with the AMV at ~5 to 11-year lead times displays same-sign patterns for almost all models (not shown). A similar lead-lagged correlation between global warming rate and the AMV is also captured in the historical simulations from the CMIP5 models (not shown). The composite (Fig. 9b) of these patterns is also roughly consistent with the observed AMV-related pattern over regions north of ~30°S (Fig. 7a) with some uncertainties evident over the North Pacific and tropical central Pacific. The actual AMV contribution to the global warming rate that is depicted by the global averaged regression coefficient ranges from -0.01 to -0.05 (°C/decade) in different CMIP5 models (not shown) compared to -0.03 (°C/decade) in the observations. In detail, the AMV in CMIP5 models

Table 2 The simultaneous and maximum lead correlation coefficient of the AMV with GMST and GWR

	AMV1	AMV2	AMV3	AMV4	AMV5	AMV6	AMV7
GMST GWR (leading year)	0.89 - 0.81 (12 year)	0.64 - 0.78 (12 year)	0.81 - 0.96 (15 year)	0.81 - 0.88 (15 year)	0.73 - 0.77 (14 year)	0.79 - 0.94 (13 year)	0.79 - 0.79 (14 year)



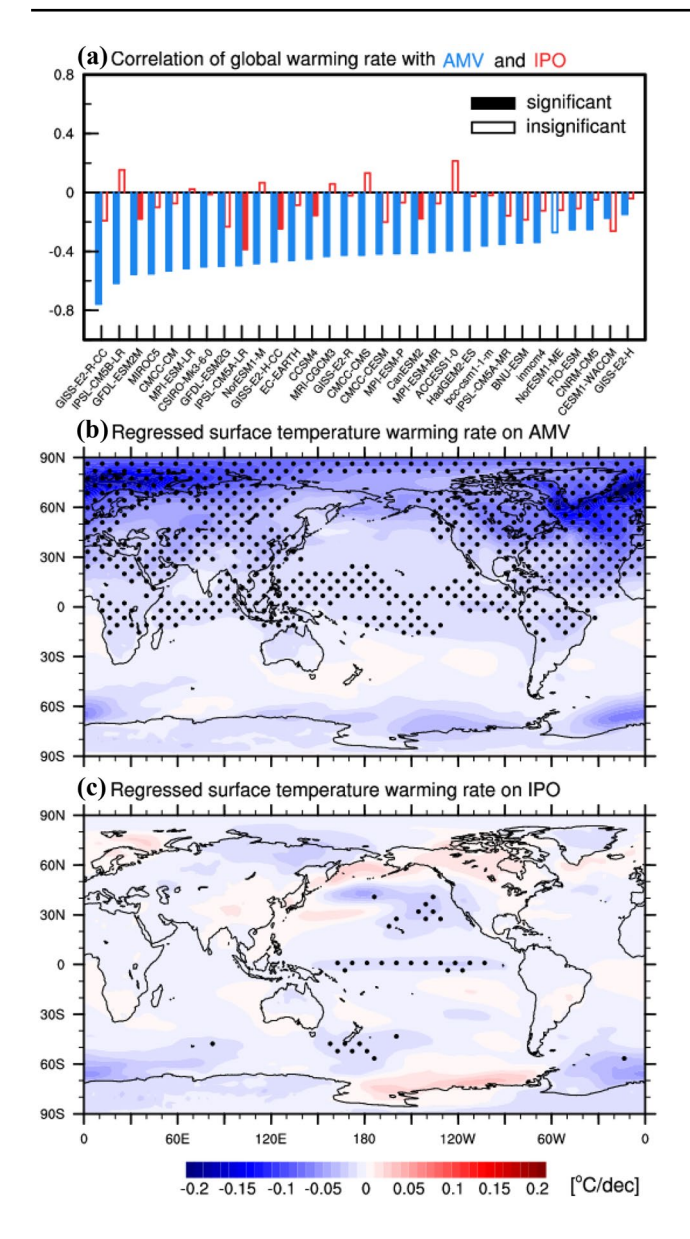


Fig. 9 a Correlation coefficients between the global warming rate with the leading AMV (the leading years are shown in Table 1; blue) and the simultaneous IPO (red) for the 31 CMIP5 models. Filled and hollow bars indicate that the correlations are significant and insignificant at the 95% significance level, respectively. **b** Multi-model ensemble mean of the regressed surface temperature warming rate (°C/decade) on the normalized AMV index (AMV lead the surface temperature warming rate by 5-11 years in different models). **c** Multi-model ensemble mean of the regressed surface temperature warming rates (°C/decade) on the normalized IPO index. Stippling indicates regions where the regression coefficients have the same sign in more than 2/3 of the models

contributes to the surface temperature of the Northern and Southern Hemisphere within a range of -0.01 to -0.07 and -0.04 to 0.008 (°C/decade), respectively. In observations, it contributes around -0.09 in the Northern Hemisphere and -0.0007 (°C/decade) in the Southern Hemisphere. The AMV associated global surface temperature changes are

likely non-negligible to the total global warming trend over recent decades. For example, the observed AMV using our methodology contributes ~25.4% to 38.8% to the global temperature trend during 1951–1980 and accounts for ~3.0 to 8.7% during 1981–2010. These values are obtained by calculating the fraction of AMV-related global-mean temperature changes (via linear regression) compared to the total global-mean temperature change during these time periods. The uncertainty range is obtained by considering different ways of defining the unforced AMV (Table 2).

In comparison, the IPO index in most of the models exhibits no statistically significant simultaneous correlations with the simulated global temperature rate variations (Fig. 9a). We also examine their lead/lag relationships and the models exhibit a large diversity for their relation. Almost all of the models show no statistically significant correlations except for 9 models (Fig. 10). The composite of regressed surface temperature rate on the normalized IPO index also shows no consistent signal except for weakly negative rates over the Pacific (Fig. 9c). This suggests that the AMV has a close relationship with natural GMST fluctuations on multidecadal timescales. In contrast, the IPO again exhibits no consistent statistical relationship with the simulated global temperature rate variations.

To further investigate whether the AMV effectively modulates the global temperature rate, we conduct a targeted model experiment with the GFDL coupled model, version 2Mc (CM2Mc). In the coupled model, a 50-year sinusoidally varying AMV-like SST anomaly is prescribed in the North Atlantic (Fig. 11). We find that the simulated global temperature rate is significantly modulated by episodes of both global warming and cooling. This idealized simulation is largely in agreement with the AMV impact on the multidecadal warming rate fluctuations seen in the observations (Fig. 12). Moreover, this idealized AMV-forced experiment produces GMST variations that are closely connected to the AMV variability. In addition, the corresponding surface warming pattern (Fig. 13) is largely consistent with the observations (Fig. 5). There are opposite signs of the simulated SST anomalies over the North Pacific as well as the tropical central and eastern Pacific, which may due to either uncertainties in the observations and/or model deficiencies in capturing the AMV signature in these regions (e.g., Zanchettin et al. 2016; Ruprich-Robert et al. 2017; Fig. 13b). We emphasize that the simulated global temperature rate is phase shifted by about 1/4 of the dominant periodicity compared with the GMST and AMV (Fig. 13a). The global mean temperature rate accordingly lags the AMV by about 14 years at the maximum correlation (Fig. 14a), which is close to the 12 years seen in the observations (Fig. 1). Correspondingly, the regressed temperature rate pattern exhibits cooling in the regions north of $\sim 30^{\circ}$ S as in the observations



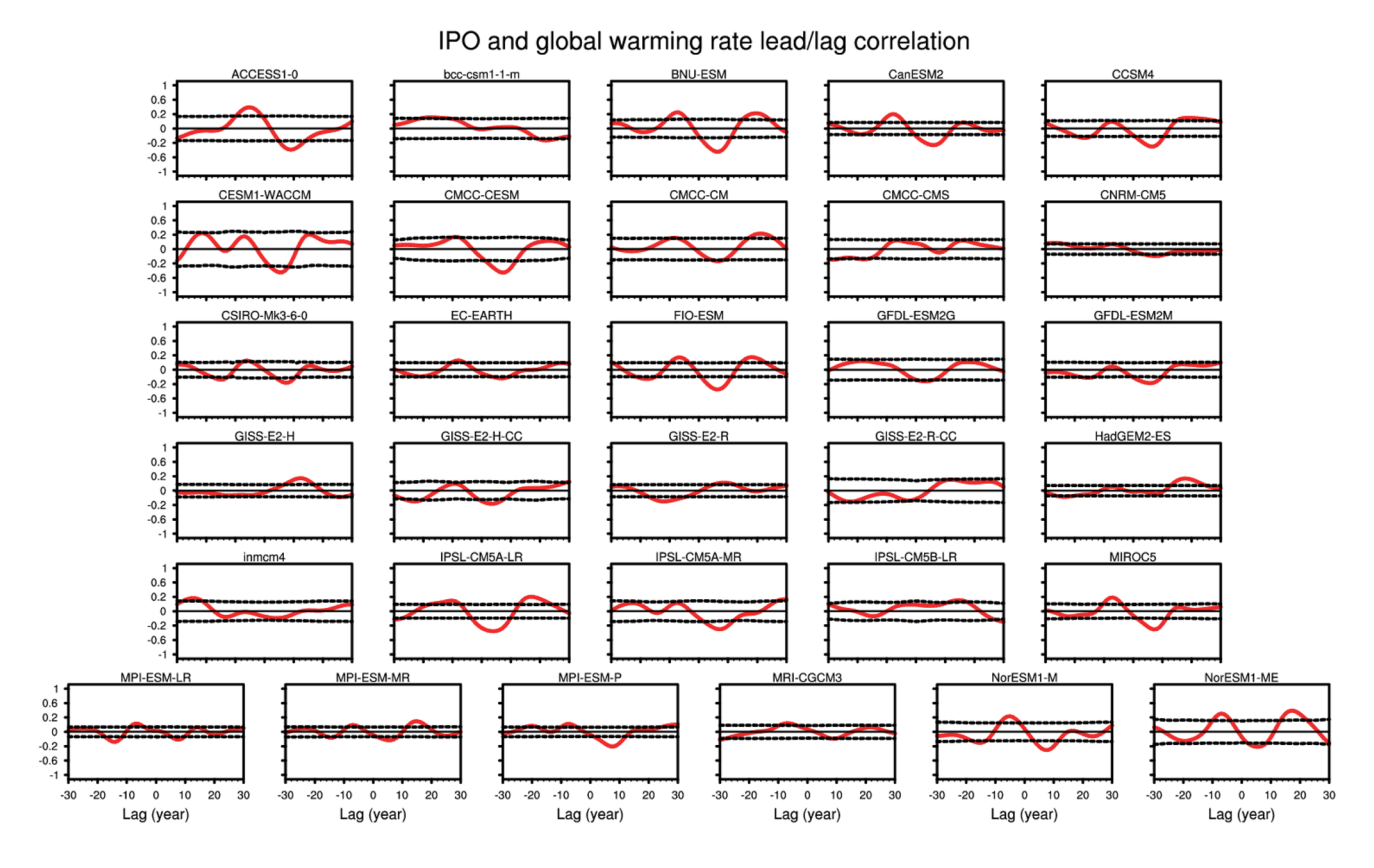


Fig. 10 Cross correlations between global warming rate and IPO in the pre-industrial control simulations from 31 CMIP5 model. Positive (negative) years on the x-axis indicate that the IPO leads (lags) the global warming rate. The dashed lines indicate the 95% confidence levels

except for the North Pacific, tropical central and eastern Pacific (Fig. 14b).

At present, no consistent argument is proposed to explain how the AMV modulates the GMST variability. Previous

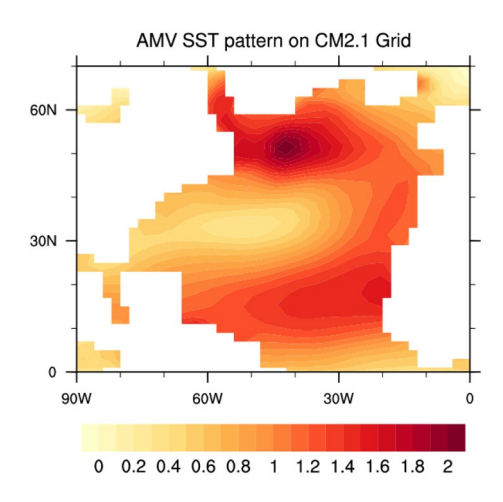


Fig. 11 The AMV-related SST anomalies that are used to force the coupled model. The pattern varies sinusoidally on a 50-year timescale

work on the role of the AMV mostly involves variations of the AMOC (e.g., Wyatt et al. 2012; Chen and Tung 2014). When the AMOC is strengthening, the ocean transports more heat poleward, increasing North Atlantic SSTs and leading to increased sea ice melt (Drijfhout et al. 2014). As the surface signature of the AMOC (Knight et al. 2005; Msadek et al. 2011), the AMV is often regarded to modulate GMST through surface heat flux changes (e.g., Wu et al. 2007; Semenov et al. 2010, 2014; Mahajan et al. 2011; Wyatt et al. 2012). Thus, we examine the relationship between anomalous net heat flux into the atmosphere and the AMV in the CMIP5 pre-industrial control simulations. The positive correlation between AMV and net heat flux indicates that net surface heat flux into the atmosphere is increased (i.e., reduced ocean heat uptake), thereby increasing GMST when the AMV is in its positive phase (Fig. 15a). It is further evidenced by our experiments (Fig. 15b), in which the surface sea temperature restoring provides additional heat fluxes into the atmosphere during a positive AMV phase. Regions north of ~30° S, especially the Northern Hemisphere are largely affected by this modulation of ocean heat uptake (Fig. 15b).



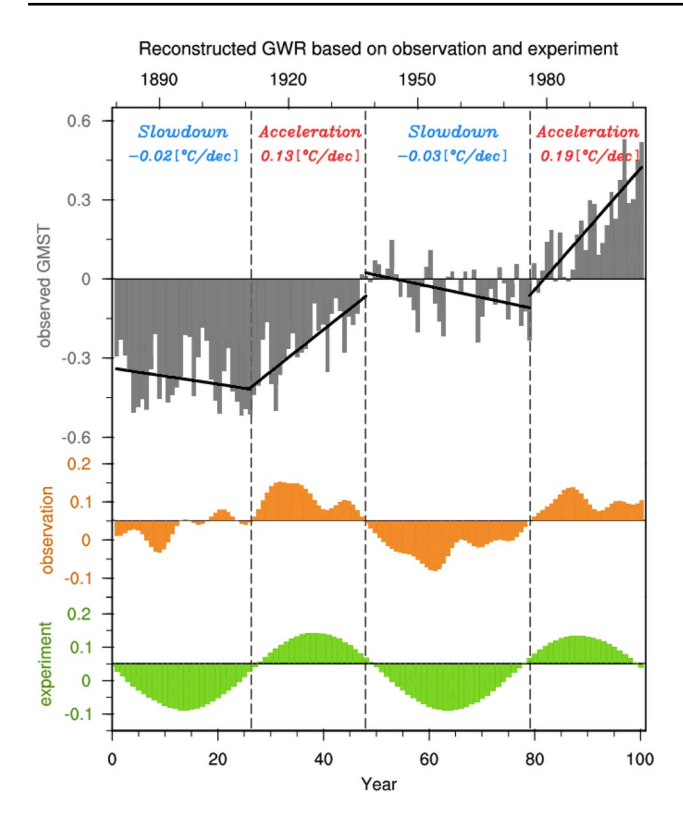


Fig. 12 Time series of the global mean surface temperature anomalies (grey in °C), global warming rate reconstructed by AMV index in the observations (orange in °C/decade, AMV leading global warming rate by 12 years) and the GFDL model experiment (green in °C/decade, AMV leading global warming rate by 14 years). The reconstructed rate is plotted relative to the mean global warming rate in 1880–2002 (0.05 °C/decade). The experimental results are multiplied by a scaling factor of 0.475, which is the ratio between observed and prescribed AMV amplitude in the model

5 Conclusions and discussion

Various factors control variations of the global warming rate about the forced long-term secular trend. The most recent decadal global warming slowdown or so-called global warming hiatus may have been caused by a combination of different mechanisms (Solomon et al. 2011; Fyfe et al. 2013; Gleisner et al. 2015; Santer et al. 2014; Medhaug et al. 2017), including tropical air-sea interactions related to the IPO (Kosaka and Xie 2013; Trenberth and Fasullo 2013; England et al. 2014; Tollefson 2014; Dai et al. 2015; Medhaug and Drange 2016), the ocean overturning circulation

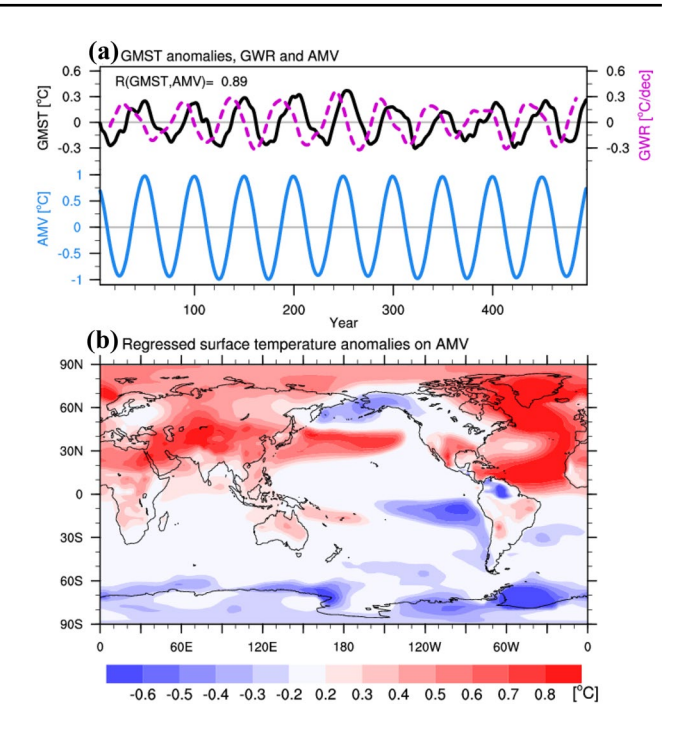


Fig. 13 a Time series of the global mean surface temperature anomalies (black line in °C), the AMV index (blue line in °C), and global warming rate (purple dashed line in °C/decade) in the CM2Mc model. b Spatial pattern for the regressed surface temperature (°C) on the simultaneous normalized AMV. Only values exceeding the 90% confidence level and examined with the FDR approach under $\alpha_{\rm FDR} = 0.1$ are shown

or remote forcing from the Atlantic (Chen and Tung 2014, 2018; Dong and Zhou 2014; McGregor et al. 2014; Li et al. 2016, Sun et al. 2018, 2019), and the combined contribution of them (Drijfhout et al. 2014; Huang et al. 2016). Different from the decadal timescale (~10 to 20 years) that is typically investigated in these studies, we here focus on longer prolonged episodes (~50 to 60 years) of global warming slow-downs and surges over the observed climate records and propose that they are possibly attributable to Atlantic multidecadal variability rather than IPO related variability. Changes in the AMV phase tend to lead global warming rate changes by around 10-20 years in observations, while the statistical relationship between the global warming rate and the IPO is far less coherent. Similar relationships can also be seen in the majority of the pre-industrial control simulations from the CMIP5 models. In addition, a climate model



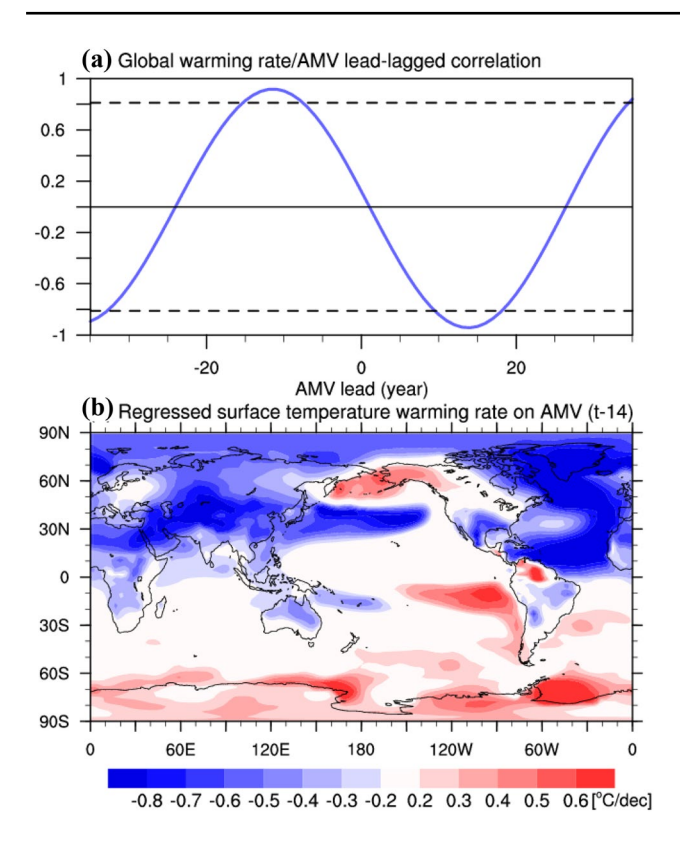


Fig. 14 a Lead-lagged correlation between the global warming rate and the AMV in the CM2Mc model and **b** regressed pattern of the global warming rate onto the AMV index (AMV is leading surface temperature warming rate by 14 years; units: °C/decade). The dashed lines in **a** indicate the 95% confidence level. Only values exceeding the 90% confidence level and examined with the FDR approach under $\alpha_{\rm FDR}\!=\!0.1$ are shown in **b**

experiment with an idealized sinusoidal AMV forcing further substantiates this conclusion. As AMV-associated SST anomalies exhibit a relatively long persistence and thus potential predictability due to their potential relationship with AMOC variability, they could be used for attribution assessments of future episodes of global warming surges and hiatuses on the multidecadal timescales.

However, there are still several issues needed to be explored further in the future. Some previous studies argued that the AMV SST index is representative of the ocean surface signature of AMOC variability rather than the oceanic heat transport, which may exhibit decadal delays with respect to SST due to oceanic dynamical inertia (e.g., Marshall et al. 2001a, b; Kravtsov et al. 2008; Frankignoul et al. 2017). Wyatt et al. (2012) argue that oceanic/atmospheric heat transport changes have a minimum/maximum about 10 years after the peak of a negative AMV phase. The related physical mechanisms of prolonged heat sequestration and heat transport changes in the ocean require further discussion. In addition, the IPO and AMV may not be independent from each other (Hu et al. 2017). There is an evident

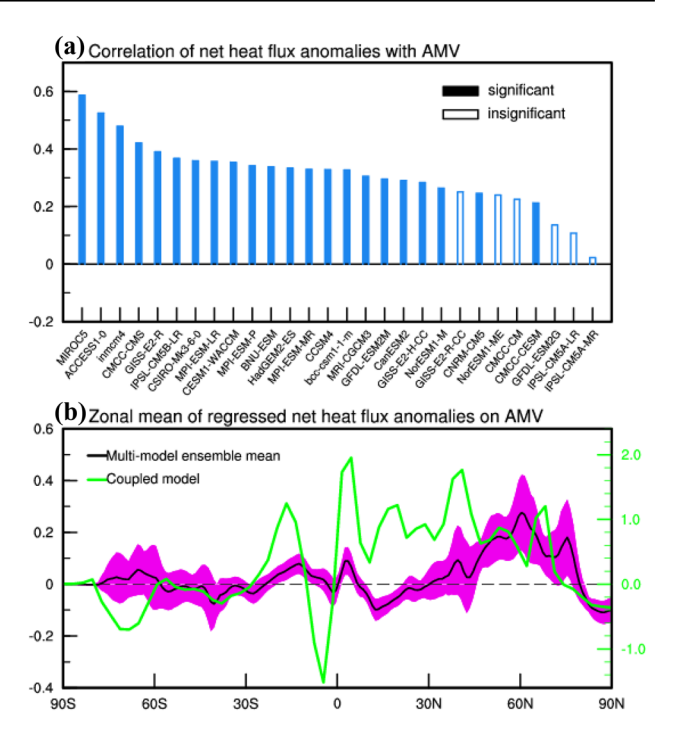


Fig. 15 a Correlation coefficients between the global mean net heat flux anomalies (positive sign denotes upward heat flux into the atmosphere) and AMV (blue) in pre-industrial control simulations from 28 CMIP5 models. Three models (EC-EARTH, FIO-ESM, and GISS-E2-H) are not included due to the heat flux data being unavailable. Filled and hollow bars indicate that the correlations are significant and insignificant at the 95% significance level, respectively. **b** Zonal mean of the regressed net heat flux anomalies (W/m²) on the normalized AMV index from the CMIP5 multi-model ensemble mean (black) and coupled model experiment (green). Shading in **b** indicates the spread (1 standard deviation) of these CMIP5 models

linear correlation between the IPO and AMV at ~ 13-year lag (D'Orgeville and Peltier 2007; Wu et al. 2011). The origin of the low frequency part of tropical Pacific decadal variability is argued to be partially caused by remote forcing from the Atlantic (Zhang and Delworth 2006; Levine et al. 2017, 2018; Sun et al. 2017). These scientific issues also deserve future research to deepen our understanding the climate variability on multidecadal timescales.

Acknowledgements The data used to reproduce the results of this paper are available by contacting the corresponding author. This study is supported by the National Key Research and Development Program (2018YFC1506002), and the National Nature Science Foundation of China (41675073). AL performed the experiments while holding a National Research Council Research Associateship Award at NOAA/PMEL. This is IPRC contribution number 1455 and SOEST contribution number 11095.

References

Bjerknes J (1964) Atlantic air–sea interaction. Advances in geophysics, vol 10. Academic Press, New York, pp 1–82



- Bjerknes J (1969) Atmospheric teleconnections from the equatorial pacific. Mon Weather Rev 97:163–172
- Booth BB, Dunstone NJ, Halloran PR, Andrews T, Bellouin N (2012) Aerosols implicated as a prime driver of twentieth-century North Atlantic climate variability. Nature 484(7393):228–232
- Chen X, Tung KK (2014) Varying planetary heat sink led to global-warming slowdown and acceleration. Science 345(6199):897-903
- Chen X, Tung KK (2018) Global surface warming enhanced by weak Atlantic overturning circulation. Nature 559(7714):387–391
- Chikamoto Y, Mochizuki T, Timmermann A, Kimoto M, Watanabe M (2016) Potential tropical Atlantic impacts on Pacific decadal climate trends. Geophys Res Lett 43(13):7143–7151
- Chylek P, Klett JD, Dubey MK, Hengartner N (2016) The role of Atlantic Multi-decadal Oscillation in the global mean temperature variability. Clim Dyn 47(9–10):3271–3279
- Clement A, Bellomo K, Murphy LN, Cane MA, Mauritsen T, Rädel G, Stevens B (2015) The Atlantic multidecadal oscillation without a role for ocean circulation. Science 350:320–324
- Cowtan K, Way RG (2014) Coverage bias in the hadcrut4 temperature series and its impact on recent temperature trends. Q J R Meteorol Soc 140(683):1935–1944
- D'Orgeville M, Peltier WR (2007) On the Pacific decadal oscillation and the Atlantic multidecadal oscillation: might they be related? Geophys Res Lett 34:L23705
- Dai A (2013) The influence of the inter-decadal Pacific oscillation on US precipitation during 1923–2010. Clim Dyn 41(3–4):633–646
- Dai A, Fyfe JC, Xie SP, Dai X (2015) Decadal modulation of global surface temperature by internal climate variability. Nat Clim Change 5(6):555–559
- Danabasoglu G, Yeager S, Kwon YO, Tribbia J, Phillips A, Hurrell J (2012) Variability of the Atlantic meridional overturning circulation in CCSM4. J Clim 25:5153–5172
- Davis ER (1976) Predictability of sea surface temperature and sea level pressure anomalies over the North Pacific Ocean. J Phys Oceanogr 6(3):249–266
- DelSole T, Tippett MK, Shukla J (2010) A significant component of unforced multidecadal variability in the recent acceleration of global warming. J Clim 24(3):909–926
- Delworth TL, Manabe S, Stouffer RJ (1993) Interdecadal variations of the thermohaline circulation in a coupled ocean-atmosphere model. J Clim 6:1993–2011
- Deser C, Phillips AS, Alexander MA (2010) Twentieth century tropical sea surface temperature trends revisited. Geophys Res Lett 37(10):L10701
- Dong L, Zhou TJ (2014) The formation of the recent cooling in the eastern tropical Pacific Ocean and the associated climate impacts: a competition of global warming, IPO, and AMO. J Geophys Res Atmos 119(19):11272–11287
- Dong B, Dai A (2015) The influence of the interdecadal Pacific oscillation on temperature and precipitation over the globe. Clim Dyn 45(9-10):2667-2681
- Dong B, Sutton RT, Scaife AA (2006) Multidecadal modulation of El Niño-Southern Oscillation (ENSO) variance by Atlantic Ocean sea surface temperatures. Geophys Res Lett. https://doi.org/10.1029/2006gl025766
- Drijfhout SS, Blaker AT, Josey SA, Nurser AJG, Sinha B, Balmaseda MA (2014) Surface warming hiatus caused by increased heat uptake across multiple ocean basins. Geophys Res Lett 41:7868–7874
- Duchon CE (1979) Lanczos filtering in one and two dimensions. J Appl Meteorol 18:1016–1022
- Enfield DB, Cid-Serrano L (2010) Secular and multidecadal warmings in the North Atlantic and their relationships with major hurricane activity. Int J Climatol 30:174–184

- Enfield DB, Mestas-Nunez AM, Trimble PJ (2001) The Atlantic multidecadal oscillation and its relation to rainfall and river flows in the continental U.S. Geophys Res Lett 28:2077–2080
- England M et al (2014) Recent intensification of wind-driven circulation in the Pacific and the ongoing warming hiatus. Nat Clim Change 4(3):222–227
- Frankcombe LM, England MH, Mann ME, Steinman BA (2015) Separating internal variability from the externally forced climate response. J Clim 28:8184–8202
- Frankignoul C, Gastineau G, Kwon YO (2017) Estimation of the SST response to anthropogenic and external forcing, and its impact on the Atlantic Multidecadal Oscillation and the Pacific Decadal Oscillation. J Clim 30:9871–9895
- Fyfe JC, von Salzen K, Cole JNS, Gillett NP, Vernier JP (2013) Surface response to stratospheric aerosol changes in a coupled atmosphere-ocean model. Geophys Res Lett 40(3):584–588
- Galbraith ED et al (2011) Climate variability and radiocarbon in the CM2Mc earth system model. J Clim 24(16):4230–4254
- Giese BS, Ray S (2011) El Niño variability in simple ocean data assimilation (SODA), 1871-2008. J Geophys Res Oceans 116:C02024
- Gleisner H, Thejll P, Christiansen B, Nielsen JK (2015) Recent global warming hiatus dominated by low-latitude temperature trends in surface and troposphere data. Geophys Res Lett 42:510–517
- Guemas V, Doblas-Reyes FJ, Andreu-Burillo I et al (2013) Retrospective prediction of the global warming slowdown in the past decade. Nat Clim Change 3(7):649–653
- Hansen J, Ruedy R, Sato M, Lo K (2010) Global surface temperature change. Rev Geophys 48:RG4004
- Henley JB et al (2015) A tripole index for the interdecadal Pacific oscillation. Clim Dyn 45(11–12):3077–3090
- Hu Z, Hu A, Hu Y (2017) Contributions of interdecadal Pacific oscillation and Atlantic multidecadal oscillation to global ocean heat content distribution. J Clim 31:1227–1244
- Huang BY et al (2015) Extended reconstructed Sea surface temperature Version 4 (ERSSTv.4). Part I: upgrades and intercomparisons. J Clim 28(3):911–930
- Huang J, Xie Y, Guan X, Li D, Ji F (2016) The dynamics of the warming hiatus over the Northern Hemisphere. Clim Dyn 48(1-2):429-446
- IPCC (2013) Summary for policymakers. In: Stocker TF, Qin D, Plattner GK et al (eds) (2013) Climate change 2013: the physical science basis. Contribution of working group I to the fifth assessment report of the intergovernmental panel on climate change. Cambridge University Press, Cambridge
- Kajtar JB, Collins M, Frankcombe LM, England MH, Osborn TJ, Juniper M (2019) Global mean surface temperature response to large-scale patterns of variability in observations and CMIP5. Geophys Res Lett 46:2232–2241
- Karl TR et al (2015) Climate change. Possible artifacts of data biases in the recent global surface warming hiatus. Science 348(6242):1469–1472
- Katsman CA, Oldenborgh GJV (2011) Tracing the upper ocean's "missing heat". Geophys Res Lett 38:L14610
- Knight JR, Allan RJ, Folland CK et al (2005) A signature of persistent natural thermohaline circulation cycles in observed climate. Geophys Res Lett 32(20):L20708
- Kosaka Y, Xie SP (2013) Recent global-warming hiatus tied to equatorial Pacific surface cooling. Nature 501(7467):403–407
- Kravtsov S, Dewar WK, Ghil M, McWilliams JC, Berloff P (2008) A mechanistic model of mid-latitude decadal climate variability. Phys D 237:584–599
- Kushnir Y (1994) Interdecadal variations in North Atlantic sea surface temperature and associated atmospheric conditions. J Clim 7:141–157



- Lee SK, Park W, Baringer MO et al (2015) Pacific origin of the abrupt increase in Indian Ocean heat content during the warming hiatus. Nat Geosci 8(6):445–449
- Levine AFZ, McPhaden MJ, Frierson DMW (2017) The impact of the AMO on multidecadal ENSO variability. Geophys Res Lett 44(8):3877–3886
- Levine AFZ, Frierson DMW, McPhaden MJ (2018) AMO forcing of multidecadal Pacific ITCZ variability. J Clim 31(14):5749–5764
- Li JP, Sun C, Jin FF (2013) NAO implicated as a predictor of Northern Hemisphere mean temperature multidecadal variability. Geophys Res Lett 40:5497–5502
- Li X, Xie SP, Gille TS, Yoo C (2016) Atlantic-induced pan-tropical climate change over the past three decades. Nat Clim Change 6:275–279
- Liu W, Xie SP, Lu J (2016) Tracking ocean heat uptake during the surface warming hiatus. Nat Commun 7:10926
- Lu R, Dong B, Ding H (2006) Impact of the Atlantic Multidecadal Oscillation on the Asian summer monsoon. Geophys Res Lett 33(24):L24701
- Mahajan S, Zhang R, Delworth TL (2011) Impact of the Atlantic Meridional Overturning Circulation (AMOC) on Arctic surface air temperature and sea ice variability. J Clim 24(24):6573–6581
- Mann ME, Steinman BA, Miller SK (2014) On forced temperature changes, internal variability, and the AMO. Geophys Res Lett 41:3211–3219
- Mann ME, Steinman BA, Miller SK (2020) Absence of internal multidecadal and interdecadal oscillations in climate model simulations. Nat Commun. https://doi.org/10.1038/s41467-019-13823
- Mantua NJ, Hare SR, Zhang Y et al (1997) A Pacific interdecadal climate oscillation with impacts on salmon production. Bull Am Meteorol Soc 78(6):1069–1079
- Marshall J, Johnson H, Goodman J (2001a) A study of the interaction of the North Atlantic Oscillation with ocean circulation. J Clim 14:1399–1421
- Marshall J, Kushnir Y, Battisti D, Chang P, Czaja A, Dickson R, Hurrell J, McCartney M, Saravanan R, Visbeck M (2001b) North Atlantic climate variability: phenomena, impacts and mechanisms. Int J Climatol 21:1863–1898
- McCarthy GD et al (2015) Measuring the Atlantic meridional overturning circulation at 26°N. Prog Oceanogr 130:91–111
- McGregor S et al (2014) Recent Walker circulation strengthening and Pacific cooling amplified by Atlantic warming. Nat Clim Change 4(10):888–892
- Medhaug I, Drange H (2016) Global and regional surface cooling in a warming climate: a multi-model analysis. Clim Dyn 46(11–12):3899–3920
- Medhaug I, Stolpe BM, Fischer ME, Knutti R (2017) Reconciling controversies about the 'global warming hiatus'. Nature 545(7652):41–47
- Meehl GA, Hu A, Santer DB, Xie SP (2016) Contribution of the interdecadal Pacific oscillation to twentieth-century global surface temperature trends. Nat Clim Change 6:1005–1008
- Morice CP, Kennedy JJ, Rayner NA, Jones PD (2012) Quantifying uncertainties in global and regional temperature change using an ensemble of observational estimates: the HadCRUT4 data set. J Geophys Res Atmos 117(D8):393–407
- Msadek R, Frankignoul C, Li LZX (2011) Mechanisms of the atmospheric response to North Atlantic multidecadal variability: a model study. Clim Dyn 36(7–8):1255–1276
- Murphy LN, Bellomo K, Cane M, Clement A (2017) The role of historical forcings in simulating the observed Atlantic multidecadal oscillation. Geophys Res Lett 44:2472–2480
- Newman M, Alexander MA, Ault TR et al (2016) The Pacific decadal oscillation. Revisited. J Clim 29(12):4399–4427

Nieves V, Willis JK, Patzert WC (2015) Recent hiatus caused by decadal shift in Indo-Pacific heating. Science 349(6247):532–535

- Parker D et al (2007) Decadal to multidecadal variability and the climate change background. J Geophys Res 112:D18115
- Power S et al (1999) Inter-decadal modulation of the impact of ENSO on Australia. Clim Dyn 15(5):319–324
- Riahi K, Rao S, Krey V, Cho C, Chirkov V, Fischer G et al (2011) RCP 8.5-A scenario of comparatively high greenhouse gas emissions. Clim Change 109:33–57
- Ruprich-Robert Y et al (2017) Assessing the climate impacts of the observed Atlantic multidecadal variability using the GFDL CM2.1 and NCAR CESM1 global coupled models. J Clim 30(8):2785–2810
- Santer B et al (2014) Volcanic contribution to decadal changes in tropospheric temperature. Nat Geosci 7(3):185–189
- Schmidt GA, Shindell DT, Tsigaridis K (2014) Reconciling warming trends. Nat Geosci 7:158–160
- Semenov VA, Latif M, Dommenget D, Keenlyside NS, Strehz A, Martin T, Park W (2010) The Impact of North Atlantic-Arctic multidecadal variability on Northern Hemisphere surface air temperature. J Clim 23(21):5668–5677
- Semenov VA, Shelekhova EA, Mokhov II, Zuevd VV, Koltermann KP (2014) Role of the Atlantic Multidecadal Oscillation in formation of seasonal air temperature anomalies in the Northern Hemisphere according to model calculations. Atmos Ocean Opt 27(3):253–261
- Solomon S et al (2011) The persistently variable "background" stratospheric aerosol layer and global climate change. Science 333(6044):866–870
- Steinman AB, Mann EM, Miller KS (2015) Atlantic and Pacific multidecadal oscillations and Northern Hemisphere temperatures. Science 347(6225):988–991
- Stolpe MB, Medhaug I, Knutti R (2017) Contribution of Atlantic and Pacific Multidecadal variability to twentieth-century temperature changes. J Clim 30(16):6279–6295
- Sun C, Kucharski F, Li JP, Jin FF, Kang IS, Ding RQ (2017) Western tropical Pacific multidecadal variability forced by the Atlantic multidecadal oscillation. Nat Commun 8:1–10
- Sun C, Li JP, Li X, Xue JQ, Ding RQ, Xie F, Li Y (2018) Oceanic forcing of the interhemispheric SST dipole associated with the Atlantic Multidecadal Oscillation. Environ Res Lett 13:074026
- Sun C, Li JP, Kucharski F, Xue JQ, Li X (2019) Contrasting spatial structures of Atlantic Multidecadal Oscillation between observations and slab ocean model simulations. Clim Dyn 52:1395–1411
- Takahashi C, Watanabe M (2016) Pacific trade winds accelerated by aerosol forcing over the past two decades. Nat Clim Change 6(8):768–772
- Ting M, Kushnir Y, Seager R, Li C (2009) Forced and internal twentieth-century SST in the North Atlantic. J Clim 22:1469–1481
- Ting M, Kushnir Y, Li C (2014) North Atlantic multidecadal SST oscillation: external forcing versus internal variability. J Mar Syst 133:27–38
- Tollefson J (2014) Climate change: the case of the missing heat. Nature 505(7483):276–278
- Trenberth KE (2015) Has there been a hiatus? Science 349(6249):691-692
- Trenberth KE, Fasullo J (2013) An apparent hiatus in global warming? Earth's Future 1(1):19–32
- Trenberth KE, Shea DJ (2006) Atlantic hurricanes and natural variability in 2005. Geophys Res Lett 33(12):285–293
- Tung KK, Zhou J (2015) Evidence for a Recurrent multi-decadal oscillation in global temperature and possible impacts on 21st century climate projections. World Sci Ser Asia-Pacific Weather Clim. https://doi.org/10.1142/9789814579933_0012



- van Oldenborgh GJ, te Raa LA, Dijkstra HA, Philip SY (2009) Frequency or amplitude dependent effects of Atlantic meridional overturning on the tropical Pacific Ocean. Ocean Sci 5:293–301
- Vose RS et al (2012) NOAA's merged land—ocean surface temperature analysis. Bull Am Meteorol Soc 93(11):1677–1685
- Wei M, Qiao F, Guo Y et al (2019) Quantifying the importance of interannual, interdecadal and multidecadal climate natural variabilities in the modulation of global warming rates. Clim Dyn. https://doi.org/10.1007/s00382-019-04955-2
- Wilks DS (2016) "The stippling shows statistically significant grid points": how research results are routinely overstated and overinterpreted, and what to do about it. Bull Am Meteorol Soc 97:2263–2273
- Wills RCJ, Armour KC, Battisti DS, Hartmann DL (2019) Oceanatmosphere dynamical coupling fundamental to the Atlantic Multidecadal Oscillation. J Clim 32:251–272
- Wu Z, Huang NE, Long SR, Peng CK (2007) On the trend, detrending, and variability of nonlinear and nonstationary time series. Proc Natl Acad Sci USA 104(38):14889–14894
- Wu S, Liu Z, Zhang R, Delworth TL (2011) On the observed relationship between the Pacific Decadal Oscillation and the Atlantic Multi-decadal Oscillation. J Oceanogr 67(1):27–35

- Wyatt MG, Kravtsov S, Tsonis AA (2012) Atlantic Multidecadal Oscillation and Northern Hemisphere's climate variability. Clim Dyn 38-929
- Young-Min Y, Soon-II A, Bin W, Jae HP (2019) A global-scale multidecadal variability driven by Atlantic multidecadal oscillation. Natl Sci Rev. https://doi.org/10.1093/nsr/nwz216
- Zanchettin D, Bothe O, Graf HF, Omrani NE, Rubino A, Jungclaus J (2016) A decadally-delayed response of the tropical Pacific to Atlantic multidecadal variability. Geophys Res Lett 43:784–792
- Zhang R, Delworth TL (2006) Impact of Atlantic multidecadal oscillations on India/Sahel rainfall and Atlantic hurricanes. Geophys Res Lett 33(17):L17712
- Zhang R et al (2013) Have aerosols caused the observed Atlantic multidecadal variability? J Atmos Sci 70(4):1135–1144

Publisher's Note Springer Nature remains neutral with regard to jurisdictional claims in published maps and institutional affiliations.

